

Supplementary Information

S-1

Nafion solution would stop at the narrow junctions because of the change in capillary pressure. At the narrow opening side of the junction, the sudden expansion to the large channel creates an angle large sufficiently high enough to stop the advancement of the Nafion meniscus, as shown in Figure S-1.

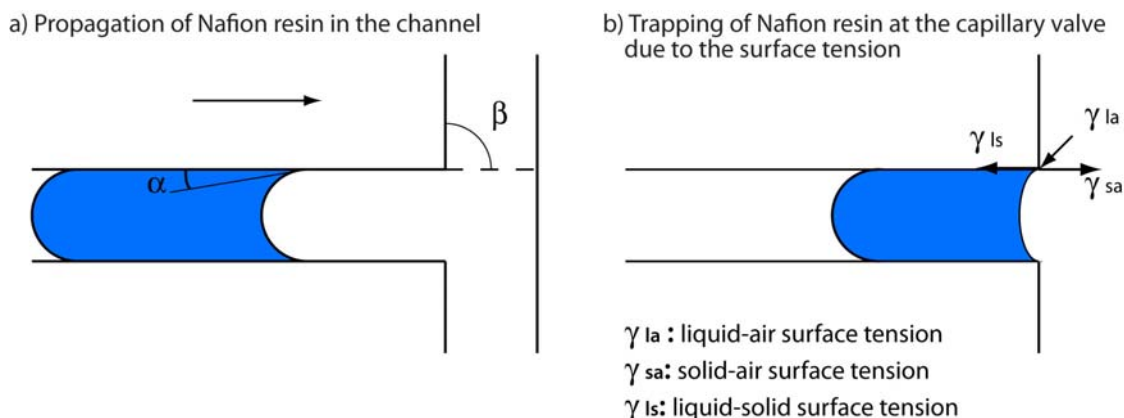


Fig. S-1 The sudden expansion in geometry creates a capillary valve that stops the flow of the Nafion resin into the neighboring channel.

According to [Zimmermann *et al.* "Valves for autonomous capillary systems", *Microfluidics Nanofluidics* (2008) 5:395-402], the pressure barrier Δp for a 2-dimensional valve can be estimated as follows:

$$\Delta p = \frac{2\gamma_{la}}{w} \left(\frac{\cos \Theta_c - \frac{\alpha}{\sin \alpha} \sin \beta}{\cos \beta + \frac{\sin \beta}{\sin \alpha} \left(\frac{\alpha}{\sin \alpha} - \cos \alpha \right)} \right) \sim 840 \text{ Pa}$$

, where w is the width of the meniscus in the valve $w = 10 \mu\text{m}$, $\gamma_{la} = 46.03\text{E}^{-5} \text{ N/cm}$ for ethanol 11.1%+ water which has a comparable composition to the Nafion resin we used, $\Theta_c = 50^\circ$ assuming the channel consists only of PDMS (in our device, one side is glass), the curvature of meniscus in the channel is $\alpha = \pi/2 - \Theta_c = 2/9\pi$, angle between the old and new microchannel wall $\beta = 90^\circ$.

S-2

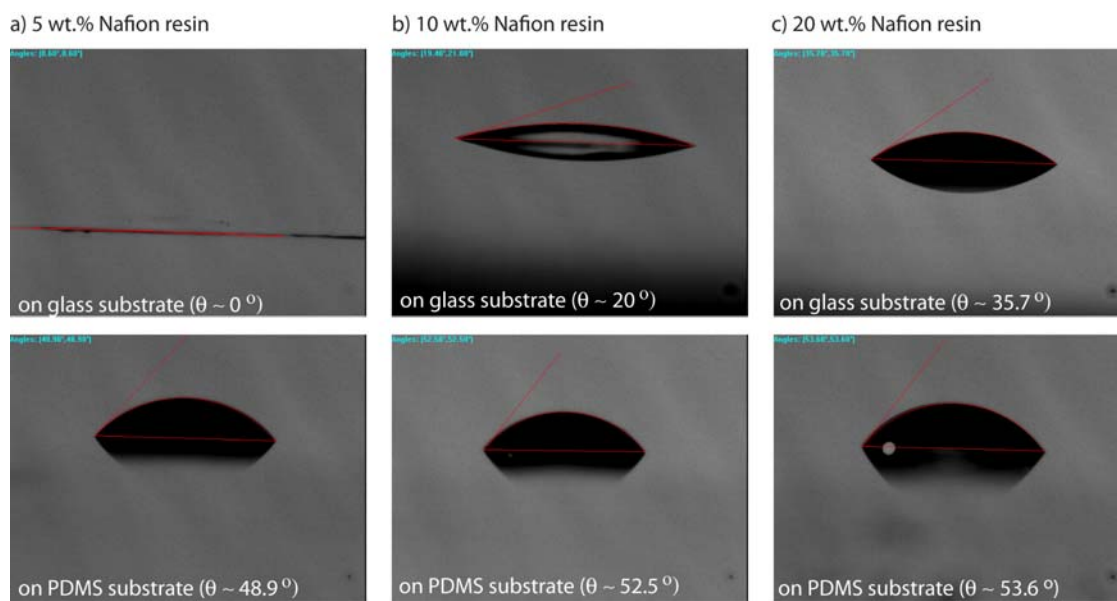


Fig. S-2 Contact angle measurement of Nafion resin with different Nafion contents on glass and PDMS substrates

S-3

We characterized the Nafion membrane junctions more carefully by measuring 1) the thickness of the membrane and 2) the I-V curves in three single gate devices. To fabricate the membranes, we used the filling and removing of 5% Nafion resin in the buffer channel (see Figure 1 a-c) of the manuscript). The result of the Nafion membrane thickness measurement is shown in Figure S-3-1. The thickness of the membrane t was varying between 20-30 μm in a 50 μm long funnel-type junction between two microchannels. The CV between the devices was $\sim 20\%$ which means that the uniformity of the membrane thickness can not be tightly controlled with the capillary valve method. Depending on the surface quality of the channel as well as on how much negative pressure is applied to the channel outlet to remove the excessive Nafion resin, the thickness of the membrane can vary.

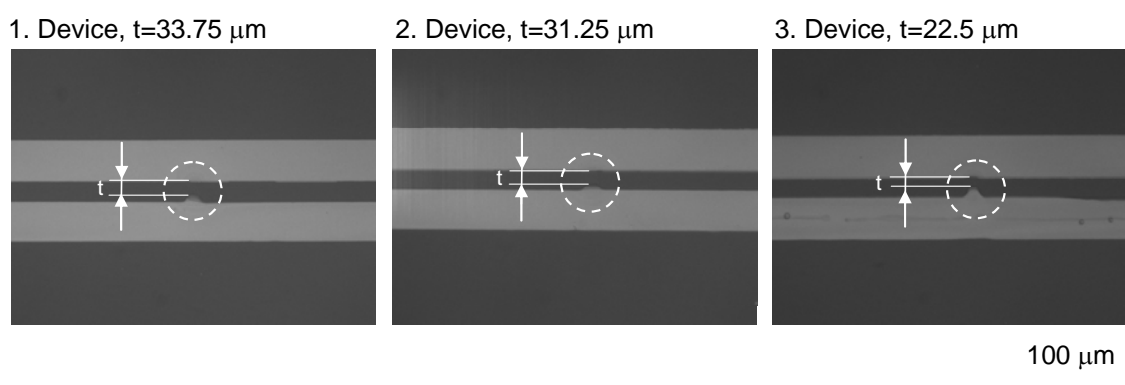


Fig. S-3-1 Measurement of the membrane thickness t

As a result of this thickness variation, the I-V measurement of these devices also showed a relatively large CV $\sim 30\%$ between the devices. For this measurement, voltage across the Nafion junction was varied from 1 to 20 V at 0.1 V increments with a delay of 10 s for each measurement point, and the current flowing through the junction was recorded at each voltage level with a Keithley SourceMeter 2400.

The measurement has been repeated on 3 different devices to quantify the uniformity of Nafion junctions across different devices. Each device was filled with 1 mM KCl buffer and was allowed to hydrate for 30 min before the measurements in order to make sure that the Nafion membrane was completely hydrated. Figure S-3-2 shows the I-V curves of three different devices and we can clearly see the characteristic linear, limiting, and overlimiting current regimes observed in a nanofluidic concentrator [Kim, S.J., Wang, Y.-C., Lee J. H., Jang, H., Han, J., "Concentration polarization and nonlinear electrokinetic flow near a nanofluidic channel", *Physical Review Letters*, 99, 044501(2007)] between 5-15 V in all three curves.

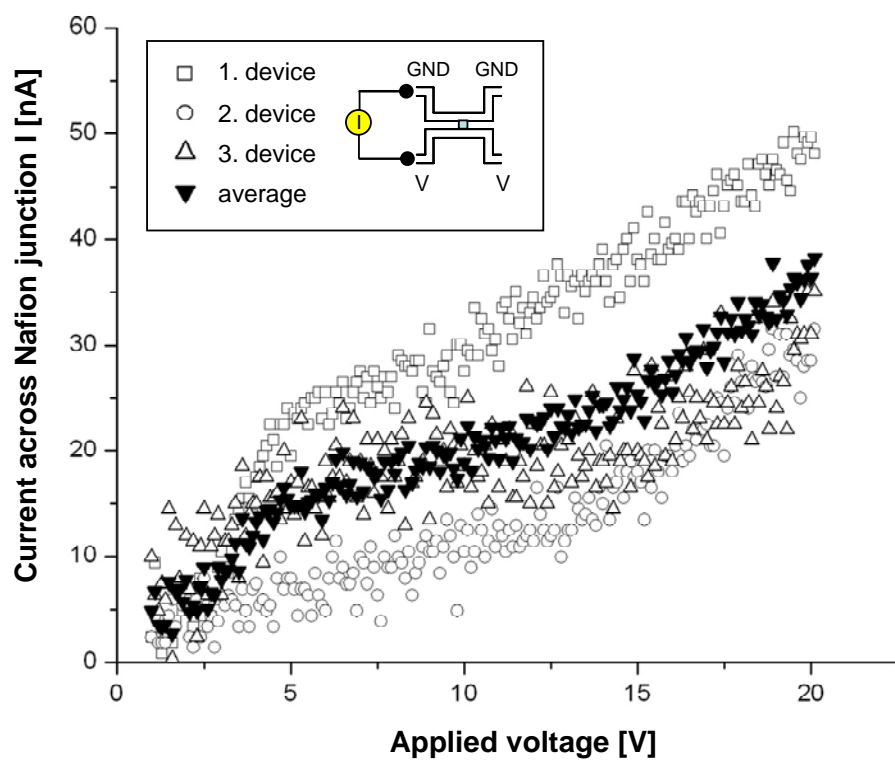


Fig. S-3-2 Measurement of I-V curves to characterize the Nafion membrane junction in single gate concentrator chips.

Compared to the filling and removing method, the alternative fabrication method based on filling and curing of the Nafion resin in separate filling channels, as described in Figure 1b of the revised manuscript, allowed better repeatability with CV <10%, as the measurement of concentration factors showed in Figure S-7.

S-4

The flow was driven by a height difference of fluids in the inlet and outlet reservoirs. The pressure difference between the two can be calculated using equation $\Delta p = \rho g(z_1 - z_2)$, where ρ is the density of the buffer solution ($9.982 \times 10^2 \text{ kg/m}^3$ for water), $g = 9.8 \text{ m/s}^2$, z_1 and z_2 are the heights of the sample solution in the inlet and outlet reservoirs. In the case of a height difference of $z_1 - z_2 = 10 \text{ mm}$, the pressure difference across the channel is $\Delta p = 98 \text{ Pa}$. The flow rate Q inside the channel can be calculated with equation 1):

$$Q = \frac{Wh^3}{12\eta L} \Delta p = \frac{Wh^3}{12\eta L} \rho g(z_1 - z_2) \quad (1)$$

, where Δp is the pressure difference across the channel, $\eta = 1 \times 10^{-3} \text{ Pa}\cdot\text{s}$ is the viscosity of water, $W = 100 \text{ }\mu\text{m}$ for channel width, $h = 10 \text{ }\mu\text{m}$ for channel depth, $L = 10 \text{ mm}$ for channel length.

In the case of $\Delta z = 10 \text{ mm}$, which was the height difference in the concentration experiment, the flow rate was $Q = 49 \text{ pL/min}$. It corresponds to $0.82 \text{ }\mu\text{m/s}$. Since the volume of the concentration plug is $\sim 10 \text{ }\mu\text{m}$ (length) $\times 10 \text{ }\mu\text{m}$ (depth) $\times 100 \text{ }\mu\text{m}$ (width) = 10 pL , the estimated concentration increase is about 5x per min. This concentration rate allows achieving a factor of 100x within 20 min. which corresponds to the concentration factor we achieved in the concentration experiment with 1x PBS buffer solution.

S-5

Since the flow speed can not be precisely controlled by a height difference to study the influence of flow speed and voltages, we performed a parameter study by using electrokinetically driven flow in 10mM phosphate buffer solution instead. The voltage difference across the sample channel ($V_{\text{diff}} = V_1 - V_2$ and $V_1 = 2V_2$, see the schematic inset in Figure S-5), which is proportional to the flow speed inside the microchannel, was varied to from 5 V to 15 V with an incremental step of 2.5 V. At the same time, the voltage difference V_{diff} determined the voltage difference across the ion-selective membrane which in turn influences the depletion force as a function of the normal field E_n across the membrane. So, with this experiment, we were able to study the influence of both flow speed and voltages.

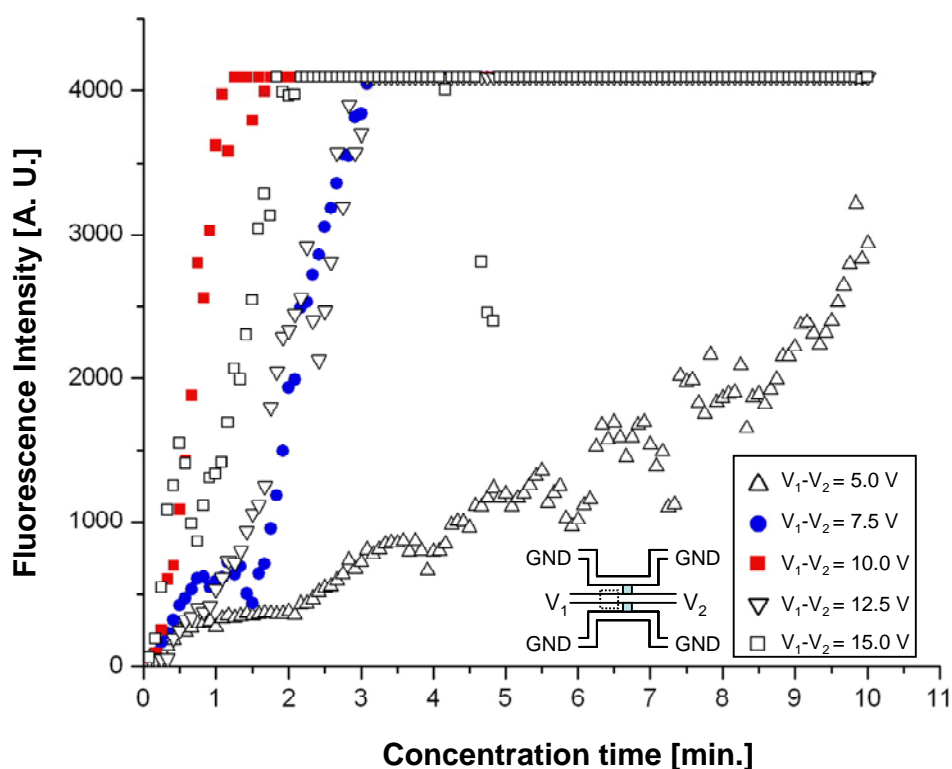


Fig. S-5 Measurement of fluorescence intensity as a function of concentration time at different voltage differences across the sample channel of a dual gate device (4 nM B-Phycoerythrin in 10 mM phosphate buffer solution, pH 7).

The result of this parameter study is shown in Figure S-5. An interesting observation was that the concentration speed increased by increasing the voltage difference up to $V_{\text{diff}} = 10$ V, as expected. By further increasing the voltage difference V_{diff} , however, the concentration speed decreased slightly and preconcentration became unstable as was

the case with $V_{\text{diff}} = 15 \text{ V}$ at $t = 5 \text{ min}$. This result shows that since the flow speed and the depletion force from the normal field are coupled with other through voltage difference V_{diff} , the equilibrium between the hydrodynamic force and depletion force can be maintained only within a limited voltage difference range. In our device, this optimal voltage difference range was between $V_{\text{diff}} = 7.5 \text{ V}$ ($V_1 = 15 \text{ V}$, $V_2 = 7.5 \text{ V}$, shown with blue circles in Figure S-5) and $V_{\text{diff}} = 10 \text{ V}$ ($V_1 = 20 \text{ V}$, $V_2 = 10 \text{ V}$, shown with red rectangles in Figure S-5). Interestingly, voltage V_1 seems to correspond to the upper limit of the limiting current regime from Figure S-3-2, which was between 15 V and 20 V.

S-6

After preconcentration-enhanced binding was completed, the channel was flushed with 1x PBS. A predetermined exposure setting (exposure time = 100 ms, 1 density filter) was used to capture an image that includes the location of the concentration zone. We used ImageJ to quantify the resulting fluorescence intensity of this zone. We defined the size of rectangular ROI (region of interest with a size of 20 pixels by 20 pixels) and placed it over the binding zone and extracted a mean fluorescence value by averaging across the pixels. Since the concentration was not uniform at both junctions, we measured the intensity values at both junctions (top and bottom) and used the higher one for the binding curve in Figure 4.

S-7

We tested three different devices with 4 nM and 400 pM B-Phycoerythrin in 10 mM phosphate buffer solution and compared the concentration rate with our previous result published in [Lee J.H., Song, Y.-A., Han, J., *Lab Chip*, 2008, 8, 597-601]. The result of the concentration experiment is shown in Figure S-7.

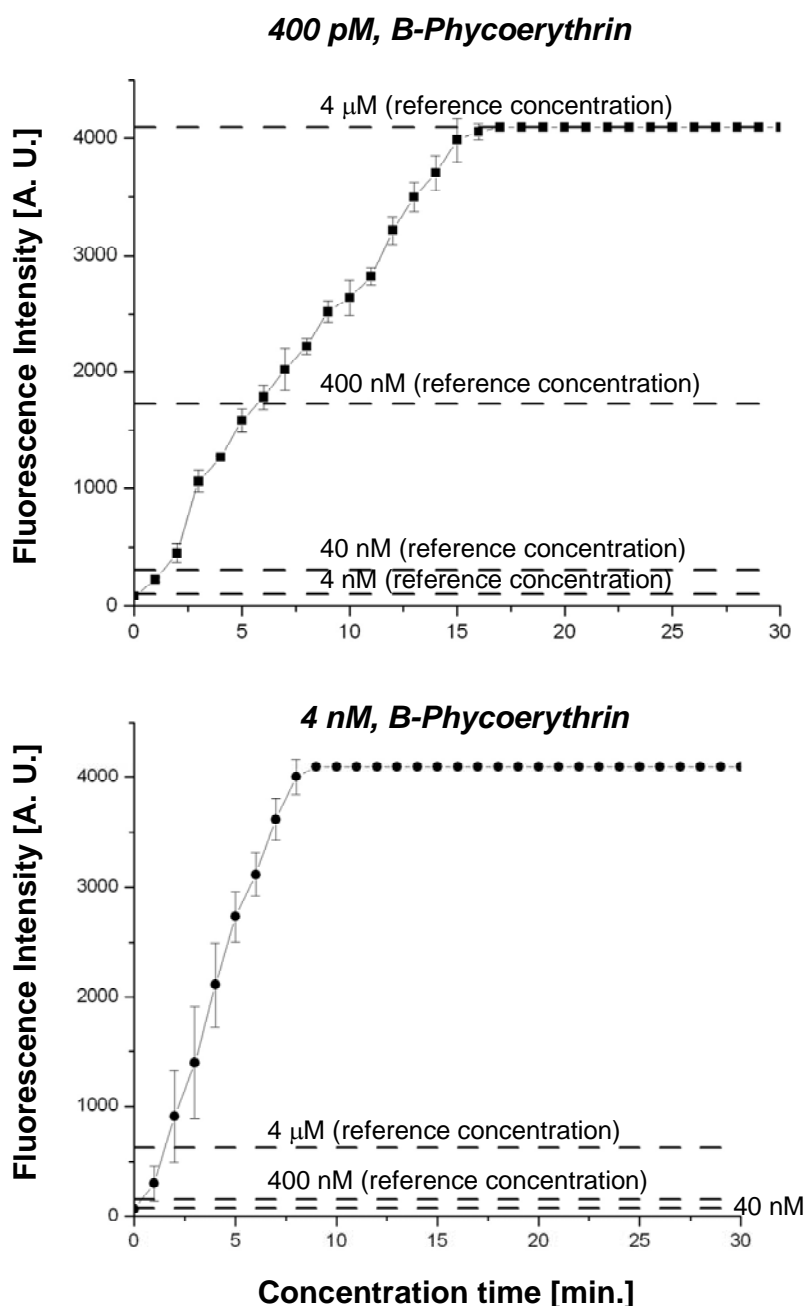


Fig. S-7 Concentration experiment in 10 mM phosphate buffer solution for two different concentrations of B-Phycoerythrin at $V_1 = V_2 = 20$ V

In the case of $c=400$ pM, we achieved a concentration factor of 1000x within 5 min. and $\sim 10^4$ x within 15 min. which compared to 5 min. of the surface-patterned Nafion membrane [Lee J.H., Song, Y.-A., Han, J., "Multiplexed proteomic sample preconcentration device using surface-patterned ion-selective membrane, *Lab Chip*, 2008, 8, 597-601] seems slower. In the case of 4 nM, we achieved 1000x within 2 min. which was comparable to that of the surface-patterned membrane. Overall, the capillary valve method allows building concentrators with a comparable performance to the surface patterning method. In addition, the low CV < 10% indicates that the filling and curing method of the Nafion resin which we used to fabricate the devices in Figure S-7 allows a better repeatability than the filling and removing method shown in Figure 1b.